AIAA JOURNAL
Vol. 31, No. 8, August 1993

Nonlinear Flutter of Orthotropic Composite Panel Under Aerodynamic Heating

Jehad F. Abbas,* R. A. Ibrahim,† and Ronald F. Gibson‡
Wayne State University, Detroit, Michigan 48202

The problem of nonlinear aerothermoelasticity of isotropic and specially orthotropic panels in supersonic airflow is examined. The Reissner functional is used with Hamilton's principle to derive the governing equations of motion, the constitutive relations, and the natural boundary conditions. The work done by aerodynamic forces is represented by using the "piston" theory for two-dimensional lifting surfaces. The aerodynamic heating effect is estimated on the basis of the adiabatic wall temperature due to the high-speed airstream. Galerkin's method is then applied to generate a set of coupled ordinary nonlinear differential equations for any number of modes. Linear flutter analysis for heated and unheated panels is carried out for the linearized six mode equations that are aerodynamically coupled. Nonlinear dynamic deflection due to the six modes is estimated for different aerodynamic pressure levels. Poincare sections are estimated for three different types of materials, and it is shown that isotropic and 90-deg orthotropic panels experience chaos whereas 0-deg orthotropic panels exhibit regular limit cycles under all possible temperature levels. The 90-deg orthotropic panels are found to exhibit flutter at lower aerodynamic pressure than the one for isotropic or 0-deg orthotropic panels. The nature of chaotic response characteristics is further examined in terms of statistical response parameters such as power spectra and probability density functions.

Introduction

THE design of space re-entry vehicles and high-speed aircraft structures requires special attention to the problem of aerothermoelasticity, which deals with the dynamic behavior of aeroelastic structures under the combined effects of aerodynamic pressures, thermodynamics, inertia forces, and elastic forces. The mathematical modeling describing the interaction between inertia forces, aerodynamic forces, aerodynamic heating, and internal stresses is not a simple task. A sharp rise in dynamic pressure and aerodynamic heating, as reflected by adiabatic wall temperature, is well recognized in high-speed flight vehicles.[1,2] Adiabatic wall temperature under these conditions can exceed the temperature limitations of the materials commonly used in aerospace structures. Much attention has been focused on the development of thermal protection systems for the surfaces of space shuttle vehicles. These systems are constructed from advanced materials such as fiber-reinforced composites.

When heat and external forces are applied simultaneously to an elastic structure, there will be a change of internal energy. Loads applied very rapidly represent nearly adiabatic conditions, whereas isothermal conditions are caused by very slowly applied loads. The principal effects of aerodynamic heating are 1) a reduction in stiffness due to softening of the matrix material (particularly for polymer matrix composite) and 2) changes in thermal stresses within the composite due to mismatch in thermal expansion coefficients of fiber and matrix materials. These effects in turn affect the flutter and dynamic response of the structure. Dynamic aerothermoelasticity includes flutter and dynamic response of aeroelastic structures to gusts and random loadings. Under large temperature gradients, the flutter speed is usually reduced when the temperature approaches the critical value, and the structure becomes dynamically unstable.

For a cantilever aircraft wing in supersonic flow, both flutter speed and the torsional vibration frequencies decrease with increasing temperature. Fung[3] considered the stability of an aerodynamically heated isotropic panel subjected to high supersonic flow on one side. In this case, for two-mode nonlinear interaction, stable static equilibrium is guaranteed for temperatures below the critical value, whereas a nontrivial limit cycle amplitude is reached for temperature rises greater than the critical value. The effect of a parabolic temperature distribution on the flutter boundary of a square panel was examined by Schaeffer and Heard.[4] They showed that the stress distribution associated with such a temperature distribution can cause a 61% reduction in the value of the critical aerodynamic pressure associated with the unheated unstressed panel. The dynamic interaction between thermal stresses and inertia forces was found[5] to depend on the natural frequency of the structure and the characteristic thermal time h^2/κ, where h is the thickness of the element (beam or plate) and κ is the thermal diffusivity of its material. The inertia effects, including the dynamic deflection, increase as the thermal time decreases.

The effects of midplane compressive stress have been investigated experimentally at different Mach numbers by several authors.[6-10] The results of these studies indicate that compressive stresses induced by aerodynamic heating could initiate flutter of a flat panel that would otherwise be stable. Furthermore, the results showed that additional heating could stop the flutter. The reversal in the flutter trend was attributed to the postbuckling behavior of panels. Guy and Bohon[11] conducted a series of experiments on two- and four-bay panels of aluminum alloy and 17-7PH stainless steel and on the actual full-scale vertical stabilizer of the X-15 airplane. These tests were conducted at a Mach number of 3.0 at various dynamic pressures and at stagnation temperature up to 660°F. All panels exhibited flutter boundaries characterized by diverse trends for the panel conditions before and after thermal buckling. In the flat unbuckled condition, the panel thickness required to prevent flutter increased with increasing thermally induced stress. Analysis of postbuckling flutter boundaries showed that, as the thermal stress increased, increasing thickness was required to prevent flutter. The peak thickness re-

Presented as Paper 92-2132 at the AIAA/ASME/ASCE/AHS/ASC 33rd Structures, Structural Dynamics, and Materials Conference, Dallas, TX, April 13-15, 1992; received July 14, 1992; revision received Dec. 10, 1992; accepted for publication Dec. 10, 1992.

*Graduate Student, Department of Mechanical Engineering.
†Professor, Department of Mechanical Engineering. Associate Fellow AIAA.
‡Professor, Department of Mechanical Engineering. Member AIAA.

quired to prevent flutter in the presence of aerodynamic heating occurs at the transition between the flat panel boundary and the buckled panel boundary. The flutter boundary for the 17-7PH stainless-steel panels was relatively unaffected by aerodynamic heating before thermal buckling. Differences in the results for the steel and aluminum panels were attributed to differences in edge rotational restraint and in the ratio of lateral to longitudinal stress in the panels.

In recent years, there has been a tremendous advancement in the science and technology of new materials that are characterized by low density, high strength, and high stiffness-to-weight ratios. Among the most commonly used materials are the fiber-reinforced composites that have been used in the aerospace and automobile industries. For composite materials, the problem of aerothermoelasticity is complicated because bending, twisting, and extensional deformations can be fully coupled in composite structures. Thus, there are significant differences in mechanical behavior between the new materials and conventional metals, and the aeroelastician must take these differences into account in mathematical modeling. A considerable amount of research work pertaining to the elastic behavior of laminated composites has been done. Since the formulation of Reissner and Stavsky[12] of the static small deflection theory of laminated plates taking into account the effect of bending-stretching coupling, a number of researchers have applied the theory to the study of bending and buckling of unsymmetric laminates and have extended the theory to the dynamic case. Bending, buckling, and vibration of various types of isotropic plates have been discussed by Leissa[13] and Szilard.[14] Bending, buckling, and vibration of laminates have been treated by Ashton and Whitney.[15] Large deflection and nonlinear free vibration of homogeneous and laminated anisotropic plates have been well documented by Chia[16] based on the von Kármán theory.

If the thickness-to-span ratio of the plate is very small (thin plates), the effects of rotary inertia and shear deformation can be neglected. The effects of orthotropicity and orientation of fibers on supersonic panel flutter based on small deflection thin plate theory were studied by Bohon,[17] Bohon and Anderson,[18] and Ketter.[19] It was found that alignment of the stiffeners parallel to the airflow would increase the critical flutter speed. It was also shown that a clamped-clamped panel can have higher critical flutter speed than the simply supported panel. Lee and Cho[20] studied the nonlinear supersonic flutter of composite panels using a finite element approach. They showed that a maximum value of the critical flutter speed is achieved when the airflow direction is aligned with the fiber orientation. The present paper examines the problem of aerothermoelasticity of isotropic and specially orthotropic panels in supersonic airflow. The aerodynamic "piston" theory is used to model the aerodynamic forces. The aerodynamic heating effect is estimated based on adiabatic wall temperature. The Reissner functional and Hamilton's principle are used to derive the governing equations of motion and natural boundary conditions. Galerkin's method is used to convert the partial differential equation of motion into a set of coupled nonlinear ordinary differential equations. In the absence of internal resonance conditions, the flutter conditions and the dynamic response of the six modes are estimated.

Mathematical Modeling

Consider a laminated panel of n layers exposed to a high-speed gas flow of velocity U_∞ as shown in Fig. 1. The axes xyz coincide with the panel geometry, whereas axes 1 and 2 are along and perpendicular to the fiber, respectively. The angle θ between the x axis and 1 axis is known as the fiber orientation. In deriving the equations of motion we will use Hamilton's principle together with the Reissner functional. The basic ingredients of Hamilton's principle are the Reissner functional, the kinetic energy, and the work done by the external and nonconservative forces. According to the first law of thermodynamics for a unit volume of the panel, the energy supplied to the element during the strain increases is $(\Delta Q + \sigma' \epsilon)$, where ΔQ is the increment of heat input, σ and ϵ are stress and strain vectors, respectively, and a prime denotes transpose. Application of the Reissner functional[21,22] gives

$$R = \int_0^a \int_0^b \frac{1}{2} [(\bar{N}_x \epsilon_{x0} + \bar{N}_y \epsilon_{y0} + \bar{N}_{xy} \gamma_{xy0}) + (\bar{M}_x \kappa_x + \bar{M}_y \kappa_y + \bar{M}_{xy} \kappa_{xy})] \, dx \tag{1}$$

where ϵ_{x0}, ϵ_{y0}, and γ_{xy0} are the midplane strains, $\bar{N}_x$ and $\bar{N}_y$ are the normal force resultants per unit length in the x and y directions, respectively, $\bar{N}_{xy}$ is the shear force resultant per unit length along the y axis in a plane perpendicular to the x axis, $\bar{M}_x$ and $\bar{M}_y$ are the bending moment resultants per unit length about the x and y axes, respectively, $\bar{M}_{xy}$ is the twisting moment resultant per unit length, κ_x and κ_y are the bending curvatures in the yz and xz planes, respectively, κ_{xy} is the twisting curvature with respect to the x and y axes, and a and b are the panel dimension defined in Fig. 1.

The stress-strain relationship for a generally orthotropic lamina is

$$\begin{Bmatrix} \sigma_x \\ \sigma_y \\ \sigma_{xy} \end{Bmatrix}_k = \begin{bmatrix} \bar{Q}_{11} & \bar{Q}_{12} & \bar{Q}_{16} \\ \bar{Q}_{12} & \bar{Q}_{22} & \bar{Q}_{26} \\ \bar{Q}_{16} & \bar{Q}_{26} & \bar{Q}_{66} \end{bmatrix}_k \begin{Bmatrix} \epsilon_x - \alpha_x \Delta T \\ \epsilon_y - \alpha_y \Delta T \\ \gamma_{xy} - \alpha_{xy} \Delta T \end{Bmatrix} \tag{2}$$

where k is the lamina number; the elements of the lamina stiffness matrix $\bar{Q}_{ij}$ depend on the lamina moduli of elasticity E_{11} and E_{22}; the lamina shear moduli of elasticity is G_{12} and the lamina Poisson ratio is ϑ_{12}; ΔT is the temperature rise due to aerodynamic heating; and α_x, α_y, and α_{xy} are the effective thermal expansion coefficients that are functions of the thermal expansion coefficients α_1 and α_2 along 1 and 2 axes of the fibers and the angle θ. These parameters are defined in the Appendix. The strain components ϵ_x, ϵ_y, and γ_{xy} are given by the nonlinear relations

$$\begin{aligned} \epsilon_x &= \frac{\partial u_0}{\partial x} + \frac{1}{2}\left(\frac{\partial w}{\partial x}\right)^2 + z\frac{\partial \psi}{\partial x} = \epsilon_{x0} + z\frac{\partial \psi}{\partial x} \\ \epsilon_y &= \frac{\partial v_0}{\partial y} + \frac{1}{2}\left(\frac{\partial w}{\partial y}\right)^2 + z\frac{\partial \beta}{\partial y} = \epsilon_{y0} + z\frac{\partial \beta}{\partial y} \\ \gamma_{xy} &= \frac{\partial u_0}{\partial y} + \frac{\partial v_0}{\partial x} + \left(\frac{\partial w}{\partial x}\right)\left(\frac{\partial w}{\partial y}\right) + z\left(\frac{\partial \psi}{\partial y} + \frac{\partial \beta}{\partial x}\right) \\ &= \gamma_{xy0} + z\left(\frac{\partial \psi}{\partial y} + \frac{\partial \beta}{\partial x}\right) \end{aligned} \tag{3}$$

where u_0 and v_0 are the displacements of the midplane along the x and y axes, respectively, $w = w(x, y, t)$ is the transverse displacement of the midplane in the z direction, and ψ and β are the angular rotations of xz and yz planes about the y and x axes, respectively.

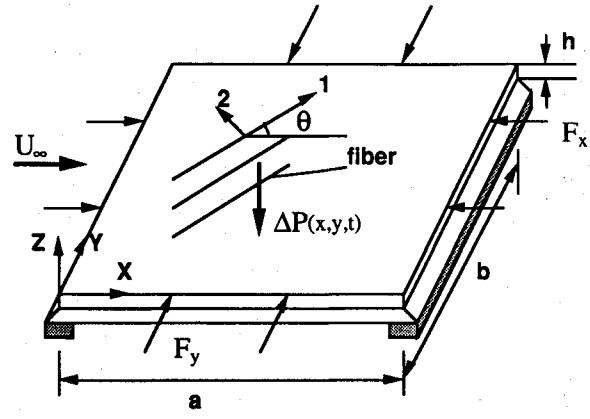

Fig. 1 Schematic diagram of a simply supported composite panel exposed to supersonic flow.

For symmetric laminates, the resultant forces and moments acting on the panel section are given by the expressions

$$\{\bar{N}\} = \int_{-h/2}^{h/2} \{\sigma\}_k \, dz, \qquad \{\bar{M}\} = \int_{-h/2}^{h/2} \{\sigma\}_k z \, dz \tag{4}$$

Substitution of Eqs. (3) into Eqs. (2) and the use of Eqs. (2) in Eqs. (4) gives the laminate constitutive relations

$$\{\bar{N}\} = [A_{ij}] \begin{Bmatrix} \epsilon_{x0} \\ \epsilon_{y0} \\ \gamma_{xy0} \end{Bmatrix} - \begin{Bmatrix} N_{xt} \\ N_{yt} \\ N_{xyt} \end{Bmatrix} \tag{5}$$

$$\{\bar{M}\} = [D_{ij}] \begin{Bmatrix} \kappa_x \\ \kappa_y \\ \kappa_{xy} \end{Bmatrix} - \begin{Bmatrix} M_{xt} \\ M_{yt} \\ M_{xyt} \end{Bmatrix} \tag{6}$$

Notice that the forces $\{\bar{N}\}$ and moments $\{\bar{M}\}$ are now functions of temperature generated by aerodynamic heating. It is also assumed that the thermoelastic coupling between the elastic deformation and the heat transfer is negligible and will be neglected. The extensional stiffness $[A_{ij}]$ and the flexural stiffnesses $[D_{ij}]$ depend on the lamina stiffnesses $\bar{Q}_{ij}$ and are given in the Appendix. The elements of the $\{N_t\}$ and $\{M_t\}$ vectors with subscript t denote those components due to aerodynamic heating and are given by the following relations:

$$\{N_t\} = \int_{-h/2}^{h/2} [\bar{Q}_{ij}]_k \{\alpha\}_k \, \Delta T \, dz \tag{5a}$$

$$\{M_t\} = \int_{-h/2}^{h/2} [\bar{Q}_{ij}]_k \{\alpha\}_k \, \Delta T \, z \, dz \tag{6a}$$

It is assumed that the panel is exposed to airflow at a constant speed for a sufficient period of time so that a steady-state condition is achieved and the adiabatic wall temperature T_{aw} can be used,[23]

$$T_{aw} = T_\infty \left(1 + \eta_r \frac{\bar{\gamma} - 1}{2} M_\infty^2\right) \tag{7}$$

where T_∞ is the freestream temperature, $\bar{\gamma}$ is the ratio of specific heat, and η_r is the recovery factor given by the expression

$$\eta_r = (T_{aw} - T_\infty)/(T_{0\infty} - T_\infty)$$

where $T_{0\infty} = T_\infty[1 + (\bar{\gamma} - 1)M_\infty^2/2]$ is the stagnation temperature, and M_∞ is the Mach number of the airstream.

The nonlinear compatibility equation of the midplane surface[24] is

$$\frac{\partial^2 \epsilon_{x0}}{\partial y^2} + \frac{\partial^2 \epsilon_{y0}}{\partial x^2} - \frac{\partial^2 \gamma_{xy0}}{\partial x \partial y} = \left(\frac{\partial^2 w}{\partial x \partial y}\right)^2 - \frac{\partial^2 w}{\partial x^2} \frac{\partial^2 w}{\partial y^2} \tag{8}$$

where the right-hand side represents nonlinear terms due to large deflection.

The kinetic energy of the panel is

$$KE = \frac{\bar{m}}{2} \int_0^a \left\{ \int_0^b \left(\frac{\partial u_0}{\partial t}\right)^2 + \left(\frac{\partial v_0}{\partial t}\right)^2 + \left(\frac{\partial w_0}{\partial t}\right)^2 + \frac{h^2}{12} \left[\left(\frac{\partial \psi}{\partial t}\right)^2 + \left(\frac{\partial \beta}{\partial t}\right)^2 \right] dy \right\} dx \tag{9}$$

where $\bar{m}$ is the mass per unit area of the panel.

The work done by external forces is given by the expression

$$W = \int_0^a \left\{ \int_0^b \Delta P w \, dy \right\} dx + \int_0^b F_x u_0 \, dy + \int_0^b F_y v_0 \, dx \tag{10}$$

where F_x and F_y are the applied in-plane static loads along the x and y directions, respectively, and ΔP is the aerodynamic pressure that is obtained by using the linear piston theory[25,28]

$$\Delta P = \frac{2q}{M} \left(\frac{\partial w}{\partial x} + \frac{1}{u_\infty} \frac{\partial w}{\partial t}\right) \tag{11}$$

where $q = \rho_\infty U_\infty^2/2$ is the dynamic pressure, and ρ_∞ is the air density.

Introducing Eqs. (1), (9), and (10) into Hamilton's principle

$$\delta \int_{t_1}^{t_2} [KE - R(u, \sigma, T) + W] \, dt = 0 \tag{12}$$

and carrying out the variational process gives the equations of motion, constitutive relations, and the natural boundary conditions. In the present analysis, both shear deformation and rotary inertia are neglected. Accordingly, the equations of motion are

$$\frac{\partial \bar{N}_x}{\partial x} + \frac{\partial \bar{N}_{xy}}{\partial y} = \bar{m} \frac{\partial^2 u_0}{\partial t^2} \tag{13}$$

$$\frac{\partial \bar{N}_y}{\partial y} + \frac{\partial \bar{N}_{xy}}{\partial x} = \bar{m} \frac{\partial^2 v_0}{\partial t^2} \tag{14}$$

$$\frac{\partial}{\partial x}\left(\frac{\partial \bar{M}_x}{\partial x} + \frac{\partial \bar{M}_{yx}}{\partial y}\right) + \frac{\partial}{\partial y}\left(\frac{\partial \bar{M}_y}{\partial y} + \frac{\partial \bar{M}_{xy}}{\partial x}\right) + \bar{N}_x \frac{\partial^2 w}{\partial x^2} + 2\bar{N}_{xy} \frac{\partial^2 w}{\partial x \partial y} + \bar{N}_y \frac{\partial^2 w}{\partial y^2} = \bar{m} \frac{\partial^2 w}{\partial t^2} - \Delta P - F_x \frac{\partial^2 w}{\partial x^2} - F_y \frac{\partial^2 w}{\partial y^2} \tag{15}$$

The constitutive relations are

$$\{\epsilon_0\} = [A_{ij}]^{-1}(\{\bar{N}\} + \{N_t\}) \tag{16a}$$

$$\{\kappa\} = \begin{Bmatrix} \dfrac{\partial \psi}{\partial x} \\ \dfrac{\partial \beta}{\partial y} \\ \dfrac{\partial \psi}{\partial y} + \dfrac{\partial \beta}{\partial x} \end{Bmatrix} = [D_{ij}]^{-1}(\{\bar{M}\} + \{M_t\}) \tag{16b}$$

where

$$\psi = -\frac{\partial w}{\partial x} \text{ and } \beta = -\frac{\partial w}{\partial y} \tag{16c}$$

and the boundary conditions are

$$F_x = \bar{N}_x - \bar{N}_{yx} \qquad \text{at } x = 0, a \tag{17a}$$

$$F_y = \bar{N}_{xy} - \bar{N}_y \qquad \text{at } y = 0, b \tag{17b}$$

$$\bar{M}_x = \bar{M}_{xy} = 0 \qquad \text{at } x = 0, a \tag{17c}$$

$$\bar{M}_y = \bar{M}_{xy} = 0 \qquad \text{at } y = 0, b \tag{17d}$$

$$\Delta P = \bar{N}_x \frac{\partial w}{\partial x} - \bar{N}_{yx} \frac{\partial w}{\partial x} + \bar{N}_{xy} \frac{\partial w}{\partial y} - \bar{N}_y \frac{\partial w}{\partial y} \quad \text{at } z = \frac{h}{2} \tag{17e}$$

Introducing the Airy stress function ϕ, whose double derivative with respect to the subscripted coordinate axes gives the resultant force $\bar{N}$ along these axes, creates

$$\{\bar{N}_x, \bar{N}_y, \bar{N}_{xy}\} = \left(\frac{\partial^2 \phi}{\partial y^{2\prime}} \frac{\partial^2 \phi}{\partial x^{2\prime}} - \frac{\partial^2 \phi}{\partial x \partial y}\right) \tag{18}$$

Now the compatibility equation, Eq. (8), can be written in terms the constitutive relation (16a) and the stress function ϕ as defined by Eq. (18)

$$g_1(\phi) + g_2(N_{xt}) + g_3(N_{yt}) + g_4(N_{xyt}) = \left(\frac{\partial^2 w}{\partial x \partial y}\right)^2 - \frac{\partial^2 w}{\partial x^2} \cdot \frac{\partial^2 w}{\partial y^2} \tag{19}$$

where the linear operators on the left-hand sides are defined as follows:

$$g_1(\phi) = \bar{A}_{22}\frac{\partial^4\phi}{\partial x^4} + (2\bar{A}_{12} + \bar{A}_{66})\frac{\partial^4\phi}{\partial x^2\partial y^2} + \bar{A}_{11}\frac{\partial^4\phi}{\partial y^4}$$

$$g_2(N_{xt}) = \bar{A}_{12}\frac{\partial^2 N_{xt}}{\partial x^2} + \bar{A}_{11}\frac{\partial^2 N_{xt}}{\partial y^2}$$

$$g_3(N_{yt}) = \bar{A}_{22}\frac{\partial^2 N_{yt}}{\partial x^2} + \bar{A}_{12}\frac{\partial^2 N_{yt}}{\partial y^2} \tag{20}$$

$$g_4(N_{xyt}) = -\bar{A}_{66}\frac{\partial^2 N_{xyt}}{\partial x\partial y}$$

and the coefficients $[\bar{A}_{ij}]$ are related to $[A_{ij}]$ as defined in the Appendix.

Equation (19) can be simplified by assuming that the thermal loading is spatially independent. In this case Eq. (19) takes the form

$$g_1(\phi) = \left(\frac{\partial^2 w}{\partial x\partial y}\right)^2 - \frac{\partial^2 w}{\partial x^2}\cdot\frac{\partial^2 w}{\partial y^2} \tag{21}$$

Using relations (16b) and (18), Eq. (15) becomes

$$g_5(\psi) + g_6(\beta) + \left(\frac{\partial^2\phi}{\partial y^2}\right)\left(\frac{\partial^2 w}{\partial x^2}\right) + \left(\frac{\partial^2\phi}{\partial x^2}\right)\left(\frac{\partial^2 w}{\partial y^2}\right) - 2\left(\frac{\partial^2\phi}{\partial x\partial y}\right) \times \left(\frac{\partial^2 w}{\partial x\partial y}\right) = \bar{m}\cdot\frac{\partial^2 w}{\partial t^2} - \Delta P - F_x\frac{\partial^2 w}{\partial x^2} - F_y\frac{\partial^2 w}{\partial y^2} \tag{22}$$

where the linear operators g_5 and g_6 are

$$g_5(\psi) = D_{11}\frac{\partial^3\psi}{\partial x^3} + (D_{21} + 2D_{66})\frac{\partial^3\psi}{\partial x\partial y^2}$$

$$g_6(\beta) = D_{22}\frac{\partial^3\beta}{\partial y^3} + (D_{12} + 2D_{66})\frac{\partial^3\beta}{\partial x^2\partial y} \tag{23}$$

Expressing ψ and β in terms of w from relations (16c), Eq. (22) takes the form

$$\bar{m}\cdot\frac{\partial^2 w}{\partial t^2} + D_{11}\frac{\partial^4 w}{\partial x^4} + 2(D_{12} + 2D_{66})\frac{\partial^4 w}{\partial x^2\partial y^2} + D_{22}\frac{\partial^4 w}{\partial y^4} - \left(F_x + \frac{\partial^2\phi}{\partial y^2}\right)\frac{\partial^2 w}{\partial x^2} - \left(F_y + \frac{\partial^2\phi}{\partial x^2}\right)\frac{\partial^2 w}{\partial y^2} + 2\frac{\partial^2\phi}{\partial x\partial y}\cdot\frac{\partial^2 w}{\partial x\partial y} - \Delta P = 0 \tag{24}$$

The constitutive equation (21), together with the equation of motion (24), completely describes the dynamic behavior of the orthotropic panel. The two equations include two unknowns, namely, the stress function ϕ and the panel deflection w.

Solution of the Stress Function

To solve Eq. (21) for the stress function ϕ, the deflection $w(x, y, t)$ may be expressed in terms of the assumed mode expansion

$$w(x, y, t) = \sum_{m=1}^{\infty}\sum_{n=1}^{\infty} W_{mn}(t)\sin(m\pi x/a)\sin(m\pi y/b) \tag{25}$$

where $W_{mn}(t)$ are the generalized coordinates.

Solution (25) satisfies the geometric boundary conditions of a simply supported panel at the four edges. Substitution of Eq. (25) into Eq. (21) gives the nonhomogeneous partial differential equation

$$\bar{A}_{22}\frac{\partial^4\phi}{\partial x^4} + (2\bar{A}_{12} + \bar{A}_{66})\frac{\partial^4\phi}{\partial x^2\partial y^2} + \bar{A}_{11}\frac{\partial^4\phi}{\partial y^4} = \frac{\pi^4}{4a^2b^2}\sum_m\sum_n\sum_r\sum_s W_{mn}(t)W_{rs}(t)ms \times \left\{(nr - ms)\left[\cos\left\{(m + r)\frac{\pi x}{a}\right\}\cos\left\{(n + s)\frac{\pi y}{b}\right\}\right] + \left[\cos\left\{(m - r)\frac{\pi x}{a}\right\}\cos\left\{(n - s)\frac{\pi y}{b}\right\}\right] + (nr + ms)\left[\cos\left\{(m + r)\frac{\pi x}{a}\right\}\cos\left\{(n - s)\frac{\pi y}{b}\right\}\right] + \left[\cos\left\{(m - r)\frac{\pi x}{a}\right\}\cos\left\{(n + s)\frac{\pi y}{b}\right\}\right]\right\} \tag{26}$$

The solution of this equation consists of two parts: the particular integral and the homogeneous solution. The particular integral may be written in the form

$$\phi_p = \frac{h\bar{E}_{11}}{4}(a/b)^2\sum_m\sum_n\sum_r\sum_s W_{mn}(t)W_{rs}(t)ms(nr - ms) \times \left\{\frac{1}{\lambda_1}\cos\left[(m + r)\frac{\pi x}{a}\right]\cos\left[(n + s)\frac{\pi y}{b}\right]\right\} + \frac{1}{\lambda_2}\left\{\cos\left[(m - r)\frac{\pi x}{a}\right]\cos\left[(n - s)\frac{\pi y}{b}\right]\right\} + \frac{h\bar{E}_{11}}{4}\left(\frac{a}{b}\right)^2\sum_m\sum_n\sum_r\sum_s W_{mn}(t)W_{rs}(t)ms(nr + ms) \times \left\{\frac{1}{\lambda_3}\cos\left[(m + r)\frac{\pi x}{a}\right]\cos\left[(n - s)\frac{\pi y}{b}\right] + \frac{1}{\lambda_4}\cos\left[(m - r)\frac{\pi x}{a}\right]\cos\left[(n + s)\frac{\pi y}{b}\right]\right\} \tag{27}$$

where the coefficients λ_i are determined by substituting Eq. (27) into Eq. (26) and equating coefficients of identical harmonics. This gives the following expressions for λ_i:

$$\lambda_1 = \frac{\bar{E}_{11}}{\bar{E}_{22}}(m + r)^2 - 2\left(\vartheta_{12} - \frac{\bar{E}_{11}}{2\bar{G}_{12}}\right)(m + r)^2 \times (n + s)^2\left(\frac{a}{b}\right)^2 + (n + s)^4\left(\frac{a}{b}\right)^4$$

$$\lambda_2 = \frac{\bar{E}_{11}}{\bar{E}_{22}}(m - r)^2 - 2\left(\vartheta_{12} - \frac{\bar{E}_{11}}{2\bar{G}_{12}}\right)(m - r)^2 \times (n - s)^2\left(\frac{a}{b}\right)^2 + (n - s)^4\left(\frac{a}{b}\right)^4$$

$$\lambda_3 = \frac{\bar{E}_{11}}{\bar{E}_{22}}(m + r)^2 - 2\left(\vartheta_{12} - \frac{\bar{E}_{11}}{2\bar{G}_{12}}\right)(m + r)^2 \times (n - s)^2\left(\frac{a}{b}\right)^2 + (n - s)^4\left(\frac{a}{b}\right)^4 \tag{28a}$$

$$\lambda_4 = \frac{\bar{E}_{11}}{\bar{E}_{22}}(m - r)^2 - 2\left(\vartheta_{12} - \frac{\bar{E}_{11}}{2\bar{G}_{12}}\right)(m - r)^2 \times (n + s)^2\left(\frac{a}{b}\right)^2 + (n + s)^4\left(\frac{a}{b}\right)^4$$

where

$$\bar{E}_{11} = E_{11}(1 - \bar{g}\Delta T), \qquad \bar{E}_{22} = E_{22}(1 - \bar{g}\Delta T)$$
$$\bar{G}_{12} = G_{12}(1 - \bar{g}\Delta T) \tag{28b}$$

$$\bar{\alpha}_1 = \alpha_1(1 - \bar{g}\Delta T), \quad \text{and} \quad \bar{\alpha}_2 = \alpha_2(1 - \bar{g}\Delta T)$$

The coefficient $\bar{g}$ measures the drop in the modulus of elasticity and the increase in the thermal expansion coefficients α_1 and α_2. In the present analysis, $\bar{g}$ is taken to be $(0.1/T_{0\infty})$, which is in good agreement with available data for the material used.[1,26]

The homogeneous solution may also be written in the form

$$\phi_h = n_1 x^2 + n_2 y^2 + n_3 xy \tag{29}$$

where the coefficients n_i are evaluated by using the in-plane boundary conditions (17), which imply zero displacements at the boundaries, i.e.,

$$\begin{Bmatrix} \langle \epsilon_{x0} \rangle \\ \langle \epsilon_{y0} \rangle \\ \langle \gamma_{xy0} \rangle \end{Bmatrix} = \frac{1}{ab}\int_0^a \int_0^b \begin{Bmatrix} \dfrac{\partial u_0}{\partial x} \\ \dfrac{\partial v_0}{\partial y} \\ \dfrac{\partial u_0}{\partial y} + \dfrac{\partial v_0}{\partial x} \end{Bmatrix} dx\, dy = \begin{Bmatrix} 0 \\ 0 \\ 0 \end{Bmatrix}$$

$$= \frac{1}{ab}\int_0^a \int_0^b \left\{ [\bar{A}_{ij}] \left[\begin{Bmatrix} \dfrac{\partial^2 \phi}{\partial y^2} \\ \dfrac{\partial^2 \phi}{\partial x^2} \\ -\dfrac{\partial^2 \phi}{\partial x \partial y} \end{Bmatrix} + \begin{Bmatrix} N_{xt} \\ N_{yt} \\ N_{xyt} \end{Bmatrix} \right] - \frac{1}{2} \begin{bmatrix} \left(\dfrac{\partial w}{\partial x}\right)^2 \\ \left(\dfrac{\partial w}{\partial y}\right)^2 \\ \left(\dfrac{\partial w}{\partial x}\right)\left(\dfrac{\partial w}{\partial x}\right) \end{bmatrix} \right\} dx\, dy = \begin{Bmatrix} 0 \\ 0 \\ 0 \end{Bmatrix} \tag{30}$$

where the symbol $\langle\,\rangle$ denotes averaging, and the coefficients n_i are

$$n_1 = \frac{h\bar{E}_{11}\pi^2}{16a^2[(\bar{E}_{11}/\bar{E}_{12}) - \vartheta_{12}^2]} \sum_m \sum_n W_{mn}^2 \times [m^2\vartheta_{12} + n^2(a/b)^2] - \tfrac{1}{2}J_1\Delta T$$

$$n_2 = \frac{h\bar{E}_{11}\pi^2}{16b^2[(\bar{E}_{11}/\bar{E}_{12}) - \vartheta_{12}^2]} \sum_m \sum_n W_{mn}^2 \times \left[\frac{m^2\bar{E}_{11}}{(a/b)^2\bar{E}_{22}} n^2\vartheta_{12}\right] - \frac{1}{2}J_2\Delta T, \qquad n_3 = 0.0 \tag{31}$$

$$J_1 = \frac{h\bar{E}_{22}(\bar{\alpha}_2 + \vartheta_{12}\bar{\alpha}_1)}{(1 - \vartheta_{12}\vartheta_{21})}, \qquad J_2 = \frac{h\bar{E}_{11}(\bar{\alpha}_1 + \vartheta_{21}\bar{\alpha}_2)}{(1 - \vartheta_{12}\vartheta_{21})}$$

Modal Dynamic Equations

Substituting the stress function solution (27) and (29) into the panel equation of motion (24) and applying Galerkin's method gives the ordinary nonlinear differential equation

$$\ddot{W}_{ij} + \frac{1}{\bar{m}}\left(\frac{4c_{ij}}{ab} + \frac{\rho U_\infty}{M}\right)\dot{W}_{ij} + \frac{\pi^2}{\bar{m}}\left\{\frac{\pi^2 i^4}{a^4} D_{11} + \frac{2\pi^2 i^2 j^2}{a^2 b^2}(D_{11}\vartheta_{21} + D_{12}) + \frac{\pi^2 j^4}{b^4} D_{22} + \left(\frac{i}{a}\right)^2 F_x + \left(\frac{j}{b}\right)^2 F_y - \frac{(1 + \vartheta_{12}\vartheta_{21})}{\pi^2\bar{m}(1 - \vartheta_{12}\vartheta_{21})}\left[\left(\frac{i}{a}\right)^2 \bar{E}_{11}\bar{\alpha}_1 + \left(\frac{j}{b}\right)^2 \bar{E}_{22}\bar{\alpha}_2\right]\Delta T\right\} W_{ij}$$

$$+ \frac{\rho_\infty U_\infty^2}{\bar{m}aM} \sum_k \frac{2ik}{i^2 - k^2}[1 - (1)^{i+k}]W_{kj} + \frac{\pi^4 h\bar{E}_{11}}{8\bar{m}a^2b^2(\bar{E}_{11}/\bar{E}_{22} - \vartheta_{12}^2)}\left(\sum_m \sum_n \left\{ i^2\left[\frac{\bar{E}_{11}}{\bar{E}_{22}}\frac{m^2}{(a/b)^2} + n^2\vartheta_{12}\right] + j^2\left[\left(\frac{a}{b}\right)^2 n^2 + m^2\vartheta_{12}\right]\right\} W_{mn}^2\right) W_{ij}$$

$$+ \frac{\pi^4 h\bar{E}_{11}}{16\bar{m}b^4} \sum_k \sum_\ell \sum_m \sum_n \sum_r \sum_s Z_{ijk\ell mnrs} W_{mn} W_{rs} W_{k\ell} = 0 \tag{32}$$

where a linear viscous damping term with coefficient c_{ij} has been introduced to account for energy dissipation. The linear stiffness expression depends on the in-plane applied forces, the aerodynamic heating, the moduli of elasticity along and perpendicular to the fiber directions, and the shear modulus of elasticity. Notice also that the parameters D_{ij} depend on temperature. The linear term in the first summation represents the aerodynamic force due to the motion of the panel. This expression results in a skew symmetric matrix that is the main source of the panel dynamic instability. The remaining expressions are nonlinear in nature and also depend on aerodynamic heating. The coefficient $Z_{ijk\ell mnrs}$ is given by the following expression:

$$Z_{ijk\ell mnrs} = ms(nr - ms)[z_{ijk\ell mnrs}(m + r, n + s) + \bar{z}_{ijk\ell mnrs}(m - r, n - s)] + ms(nr + ms) \times [z_{ijk\ell mnrs}(m + r, n - s) + z_{ijk\ell mnrs}(m - r, n + s)] \tag{33}$$

where

$$z_{ijk\ell mnrs}(M, N) = \{2MNk\ell[\delta(i + k, M) + \delta(i - k, M)][\delta(j + \ell, N) + \delta(j - \ell, N) - (N^2k^2 + M^2\ell^2)[\bar{\delta}(i + k, M) - \bar{\delta}(i - k, M)][-\bar{\delta}(j + \ell, N) - \bar{\delta}(j - \ell, N)]/[(M^4/C^2) - C_6M^2N^2 + (a/b)^4N^4]$$

$$\bar{z}_{ijk\ell mnrs}(M, N) = \begin{cases} 0, & M = N = 0 \\ z_{ijk\ell mnrs}(M, N), & \text{otherwise} \end{cases}$$

$$\delta(J, K) = \begin{cases} 1, & J = K \neq 0 \\ -1, & J = -K \neq 0 \\ 0, & \text{otherwise} \end{cases}, \quad \bar{\delta}(J, K) = \begin{cases} 2, & J = K = 0 \\ 1, & J = K \neq 0 \\ 1, & J = -K \neq 0 \\ 0, & \text{otherwise} \end{cases}$$

$$C_2 = \frac{D_{22}}{D_{11}} = \frac{E_{22}}{E_{11}}, \qquad C_6 = 2\left(\vartheta_{12} - \frac{\bar{E}_{11}}{2G_{12}}\right)$$

Introducing the following parameters,

$$\tau = t\sqrt{D_{11}/\bar{m}a^4}, \quad y_{ij} = W_{ij}/h, \quad \lambda = \rho_\infty u_\infty^2 a^3/(MD_{11})$$

$$R_x = F_x a^2/D_{11}, \quad R_y = F_y a^2/D_{11}, \quad \mu = \rho_\infty a/\bar{m}$$

$$A_{mn} = [m^2b^2/(C_2a^2) + n^2\vartheta_{12}], \quad \zeta = \sqrt{\mu/M}$$

$$B_{mn} = (na/b)^2 + m^2\vartheta_{12}$$

$$R_{Yt} = \frac{h\bar{E}_{22}\bar{\alpha}_2}{\pi^2 D_{11}} a^2\Delta T, \quad R_{xt} = \frac{h\bar{E}_{11}\bar{\alpha}_1}{\pi^2 D_{11}} a^2\Delta T \tag{34}$$

$$C_1 = \vartheta_{21} + (D_{12}/D_{11}), \quad C_3 = (1 + \vartheta_{12}\vartheta_{21})/(1 - \vartheta_{12}\vartheta_{21})$$

$$C_4 = 1.5\,\pi^4(a/b)^2C_2, \quad C_5 = 0.75(1 - \vartheta_{12}\vartheta_{21})\pi^4(a/b)^4$$

$$\bar{\omega}_{ij}^2 = \pi^4[i^4 + 2C_1i^2j^2(a/b)^2 + C_2(a/b)^2j^4] + \pi^2\{i^2R_x + j^2R_y(a/b)^2 - C_3[i^2R_{xt} + j^2(a/b)^2R_{yt}]\}$$

Equation (32) takes the nondimensional form

$$y''_{ij} + (\zeta_{ij} + \zeta\sqrt{\lambda})y'_{ij} + \bar{\omega}^2_{ij}\, y_{ij} + \lambda \sum_{k=1} \frac{2ik}{i^2 - k^2} [1 - (-1)^{i+k}]\, y_{kj}$$
$$+ C_4 \sum_{m=1} \sum_{n=1} (i^2 A_{mn} + j^2 B_{mn})\, y^2_{mn}\, y_{ij}$$
$$+ C_5 \sum_{k=1} \sum_{\ell=1} \sum_{m=1} \sum_{n=1} \sum_{r=1} \sum_{s=1} Z_{ijk\ell mnrs}\, y_{mn}\, y_{rs}\, y_{k\ell} = 0 \quad (35)$$

Equation (35) can also be used for the isotropic case by assigning the same moduli of elasticity in directions 1 and 2, i.e.,

$$D_{11} = D_{22} = D = \frac{\bar{E}h^3}{12(1 - \vartheta^2)}, \qquad D_{12} = \vartheta D$$
$$\vartheta_{12} = \vartheta_{21} = \vartheta, \qquad \bar{G}_{12} = \bar{G} = \frac{\bar{E}}{2(1 + \vartheta)} \quad (36)$$

Linear Flutter Analysis

The temperature-dependent mechanical properties of several isotropic and graphite/epoxy composite materials have been documented by Houbolt[2] and by Sun and Chen,[26] respectively. These are used to determine the stability and response of a panel made of steel and panels made of unidirectional graphite/epoxy with 0- and 90-deg fiber orientation. Equation (35) is the general equation of motion of mode ij that is coupled linearly through aerodynamic forces and nonlinearly through stiffness in-plane stretching forces with other modes. In the absence of airflow, the linear coupling vanishes and Eq. (35) constitutes an autonomous set of nonlinear differential equations. The dynamic behavior of the plate under small initial conditions becomes significant in the neighborhood of internal resonance conditions. Chang et al.[27] considered this problem and showed that there exist various combinations of two different linear modes that are in 1:1 internal resonance for specific values of the aspect ratio a/b. Figure 2 shows a plot of the panel natural frequencies against aspect ratio for zero airflow and constant temperature. The flutter of the panel in the neighborhood of internal resonance will be considered in another paper. However, linear flutter analysis can

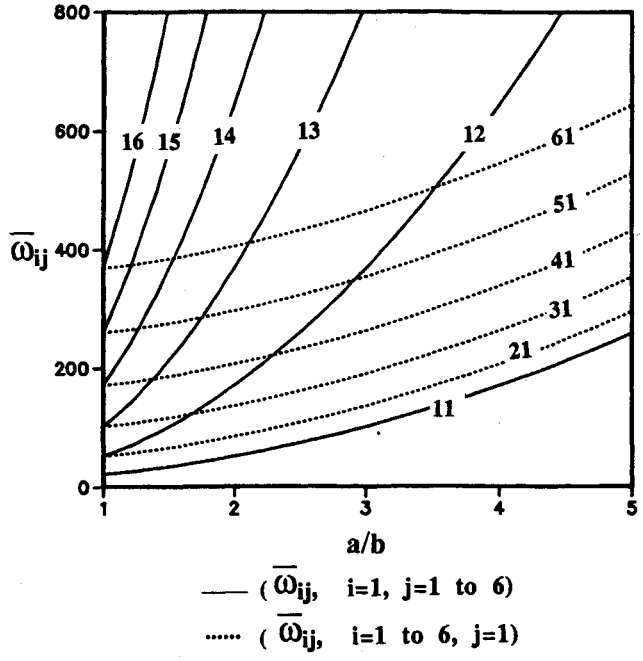

Fig. 2 Natural frequencies of an unheated isotropic panel at zero airflow velocity: ——, ω_{ij}, $i = 1, j = 1, 2, \ldots, 6$; · · · ·, ω_{ij}, $i = 1, 2, \ldots, 6, j = 1$.

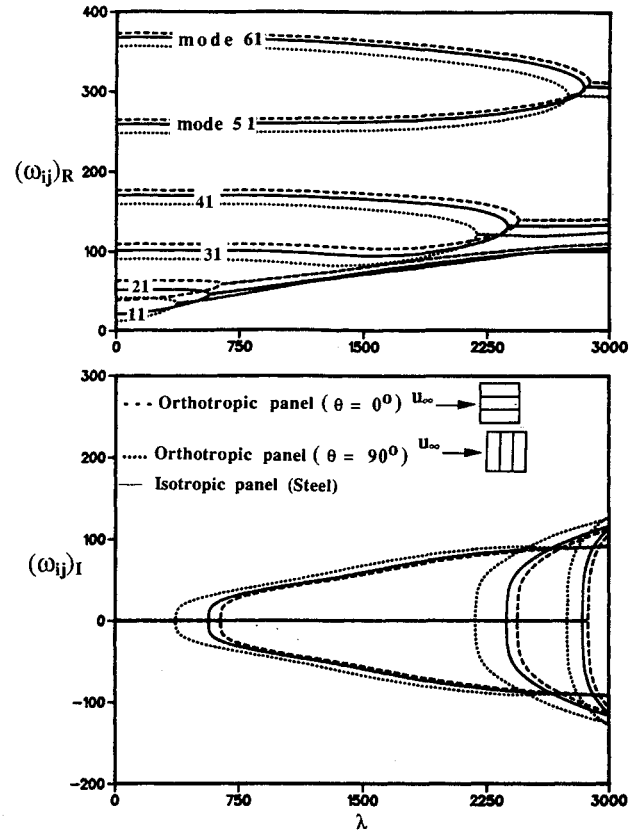

Fig. 3 Natural frequencies $(\omega_{ij})_R$ showing coalescence and damping measure $(\omega_{ij})_I$ of aeroelastic modes of unheated panel: ——, isotropic panel (steel); - - - -, orthotropic panel $\theta = 0$ deg; · · · ·, orthotropic panel $\theta = 90$ deg.

be determined from the eigenvalues of the linear part of Eq. (35) by introducing the solution

$$y_{ij}(\tau) = Y^0_{ij} \exp(i\omega\tau) \quad (37)$$

where ω is, in general, a complex number $\omega = \omega_R + i\omega_I$; $T_{0\infty} = 390°\text{R}$, $\mu = 0.1$, $a/b = 1$, and $a/h = 125$; $F_x = 0$, $F_y = 0$, and $\zeta_{ij} = 0$ are used in the present results. The real part ω_R is usually close to the normal mode natural frequencies of the panel in the absence of aerodynamic damping, whereas the imaginary values ω_I characterize the aerodynamic damping. These eigenvalues depend on the aerodynamic pressure parameter λ, aerodynamic heating, and material properties. Early studies[24] showed that accurate results are obtained for the discretized model if one considers six modes or more in the analysis. The natural frequencies were computed numerically by using the International Mathematical and Statistical Library (IMSL) subroutine eigenvalue solver of real general matrices (EVLRG). Figure 3 shows the dependence of both real and imaginary parts of the eigenvalues of the six modes, $ij = 11$ and 21–61, on the aerodynamic pressure for unheated panels. The natural frequencies are plotted for three types of materials: isotropic (steel) and orthotropic (graphite/epoxy) with fiber orientations of $\theta = 0$ and 90 deg. It is seen that the effect of aerodynamic damping is almost negligible for aerodynamic pressures less than a critical value λ_{cr}. When $\lambda > \lambda_c$ the panel becomes dynamically unstable, since the conjugate part appears as the positive real part in the solution (37). At the critical value λ_{cr}, the real parts of two modes, $ij = 11$ and 21, coalesce. This frequency merging is typical of coupled mode flutter. As expected, orthotropic panels with fiber orientation of $\theta = 90$ deg are prone to flutter at lower aerodynamic pressure than isotropic or 0-deg orthotropic panels. For heated panels the real and imaginary values of ω are shown in Fig. 4. For simply supported panels, it is seen that the aerody-

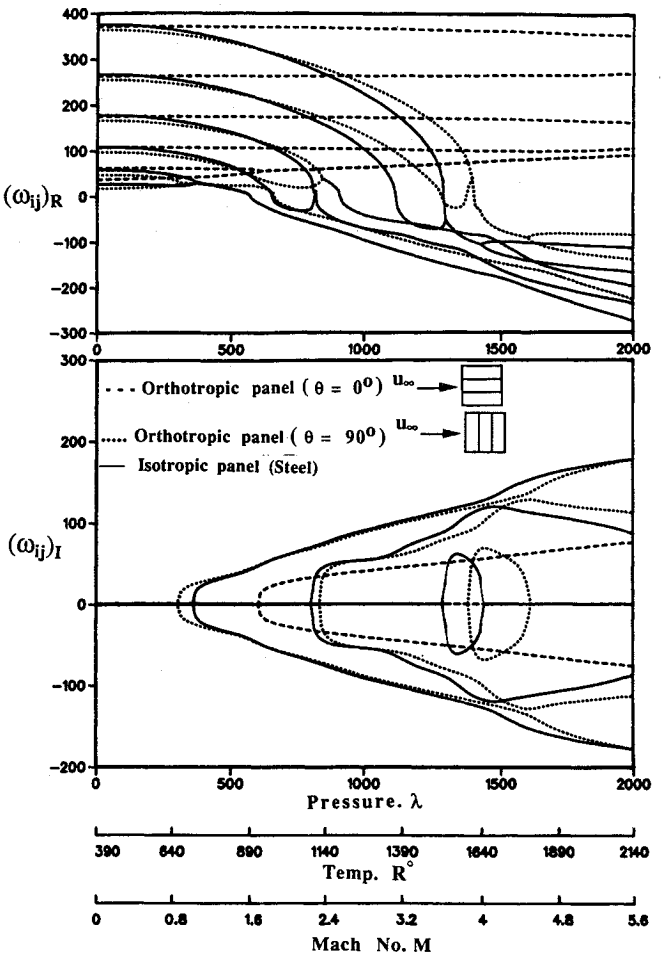

Fig. 4 Natural frequencies $(\omega_{ij})_R$ showing coalescence and damping measure $(\omega_{ij})_I$ of aeroelastic modes of a panel under aerodynamic heating: ——, isotropic panel (steel); ----, orthotropic panel $\theta = 0$ deg; · · · ·, orthotropic panel $\theta = 90$ deg.

namic heating reduces the flutter speed. For example, the critical aerodynamic pressure for the unheated panel is close to 590 whereas for the heated panel it is close to 377 for the isotropic panel. Another remarkable feature is the deformed curves of the eigenvalues of the heated panel. In the cases of both heated and unheated panels, the performance of the orthotropic panel with $\theta = 0$ deg is superior to the other cases, since it has higher critical flutter speed.

Nonlinear Response

The linear flutter analysis provides information regarding the airflow speed at which the panel becomes dynamically unstable and the amplitude of oscillation grows exponentially with time. In reality, as the amplitude increases to a certain level, the nonlinear effects become dominant and the amplitude may reach a bounded value defined by a limit cycle. In view of the multidimensionality of the nonlinear interacting modes represented by Eq. (35), analytical techniques such as harmonic balance, perturbation techniques, and averaging methods are not used. It is well known among aeroelasticians that nonlinear flutter analysis can be accomplished by considering at least the first six modes.[24] For this reason, the response of the panel is determined by numerically integrating the six nonlinear differential equations of modes, $ij = 11$ and 21-61, as generated from Eq. (35). The direct numerical integration of the six coupled nonlinear differential equations is performed by using the IMSL-DIVPAG subroutine (double precision initial-value problem solver, ADAMS-Moulton or gear method).

The time history records for the six modes, $ij = 11$ and 21-61, were obtained at different aerodynamic pressures for isotropic, 0-, and 90-deg orthotropic heated panels as shown in Figs. 5-9. Each figure contains six time history records corresponding to the six modes estimated at panel location $(x, y) =$

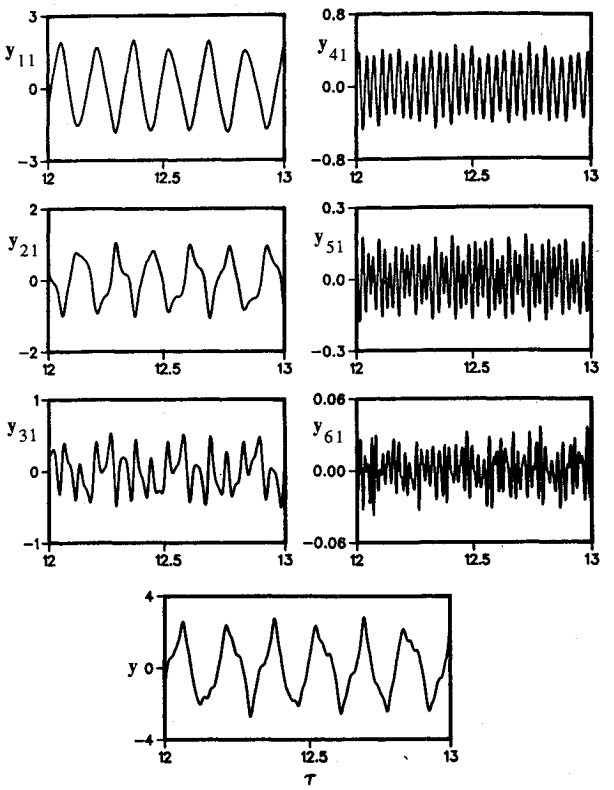

Fig. 5 Samples of time history records of the six modes and the total panel response at x, $y = 0.75a$ and $0.5b$ for a heated isotropic panel ($T = 965°$R, $M = 1.85$, $\lambda = 665$).

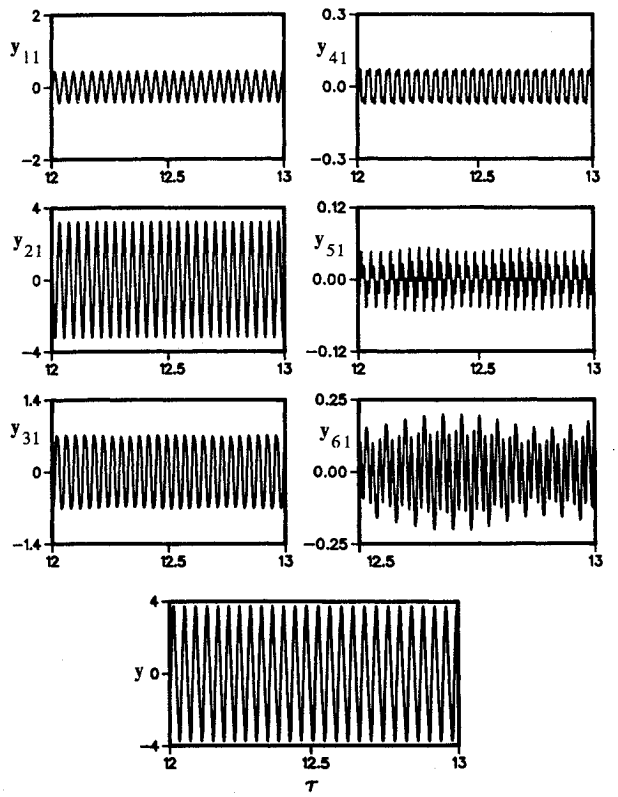

Fig. 6 Samples of time history records of the six modes and the total panel response at x, $y = 0.75a$ and $0.5b$ for a heated isotropic panel ($T = 1105°$R, $M = 2.25$, $\lambda = 795$).

0.75*a*, 0.5*b*, where the maximum deflection of the panel takes place. The resultant of the six records is plotted in the seventh plot. For isotropic heated panels, the motion first begins with period doubling, higher period order, and then random as shown in Fig. 5. Development of chaos is observed as the aerodynamic pressure increases where the heated panel ap-

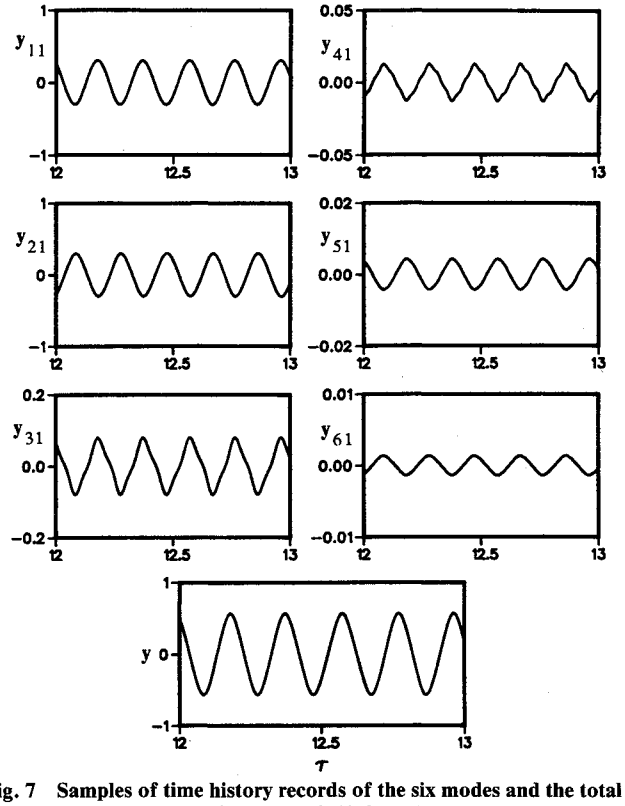

Fig. 7 Samples of time history records of the six modes and the total panel response at x, $y = 0.75a$ and $0.5b$ for a heated isotropic panel ($T = 745°$R, $M = 1.15$, $\lambda = 395$).

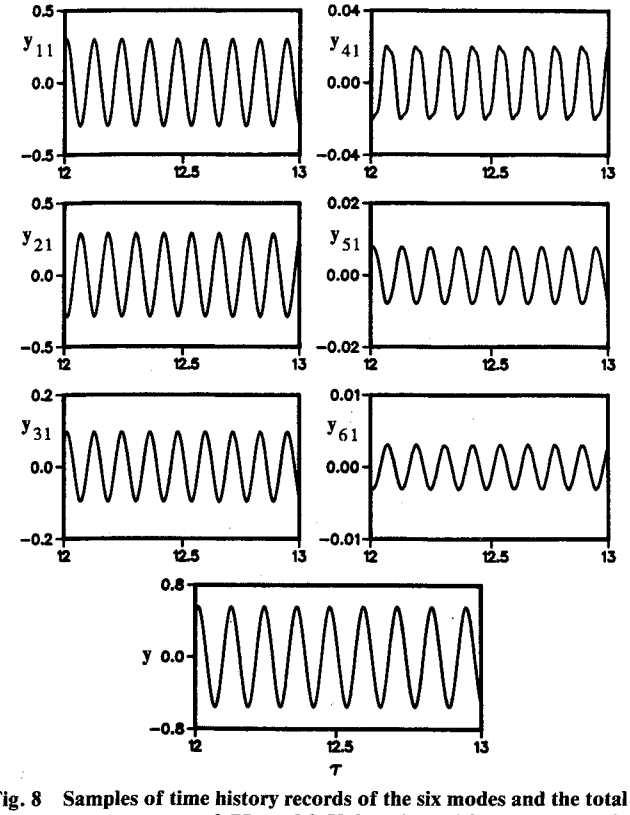

Fig. 8 Samples of time history records of the six modes and the total panel response at x, $y = 0.75a$ and $0.5b$ for a heated 0-deg orthotropic panel ($T = 990°$R, $M = 1.8$, $\lambda = 680$).

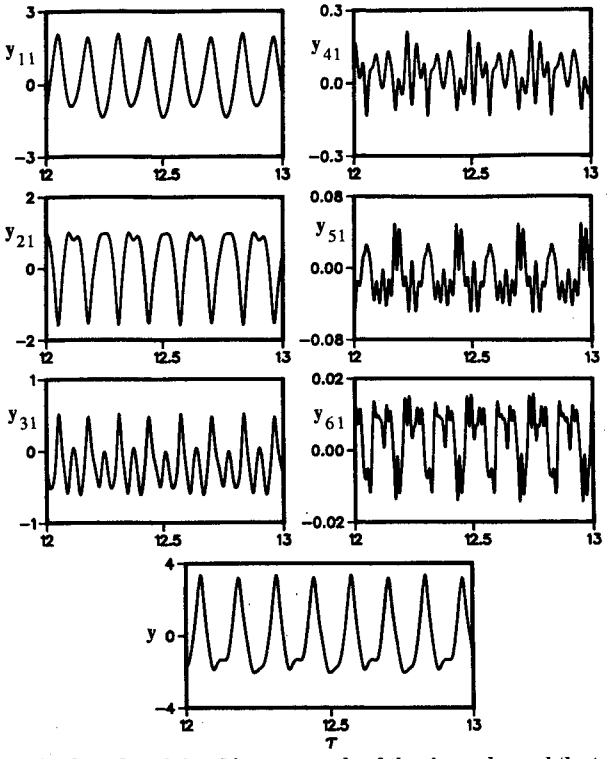

Fig. 9 Samples of time history records of the six modes and the total panel response at x, $y = 0.75a$ and $0.5b$ for a heated 90-deg orthotropic panel ($T = 1030°$R, $M = 2.05$, $\lambda = 760$).

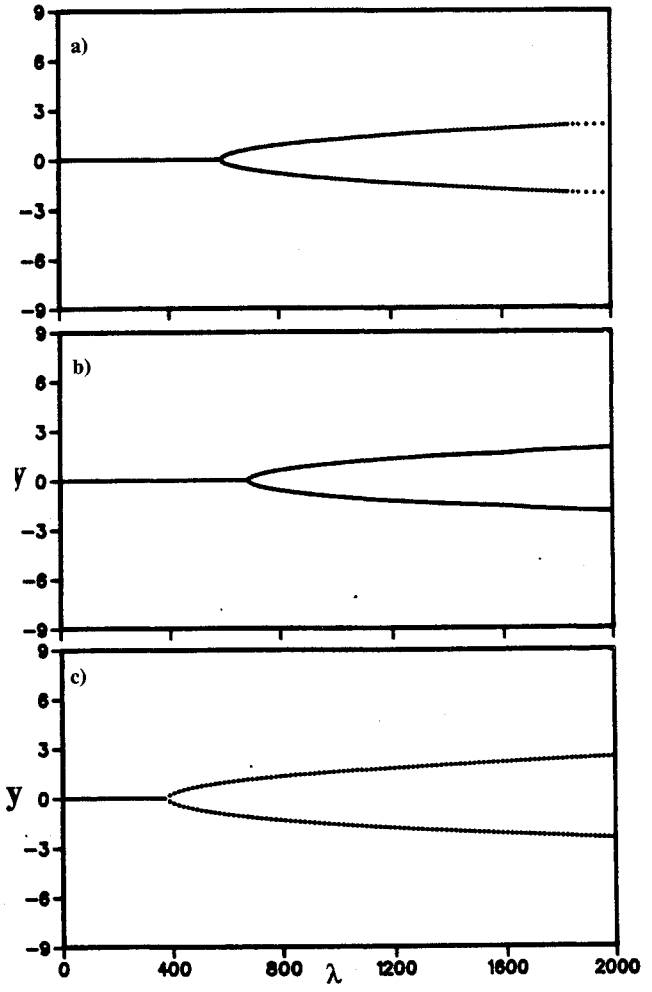

Fig. 10 Poincare sections of the first return as estimated by numerical integration for three different unheated panels: a) isotropic panel (steel); b) orthotropic panel (graphite/epoxy) $\theta = 0$ deg; and c) orthotropic panel (graphite/epoxy) $\theta = 90$ deg.

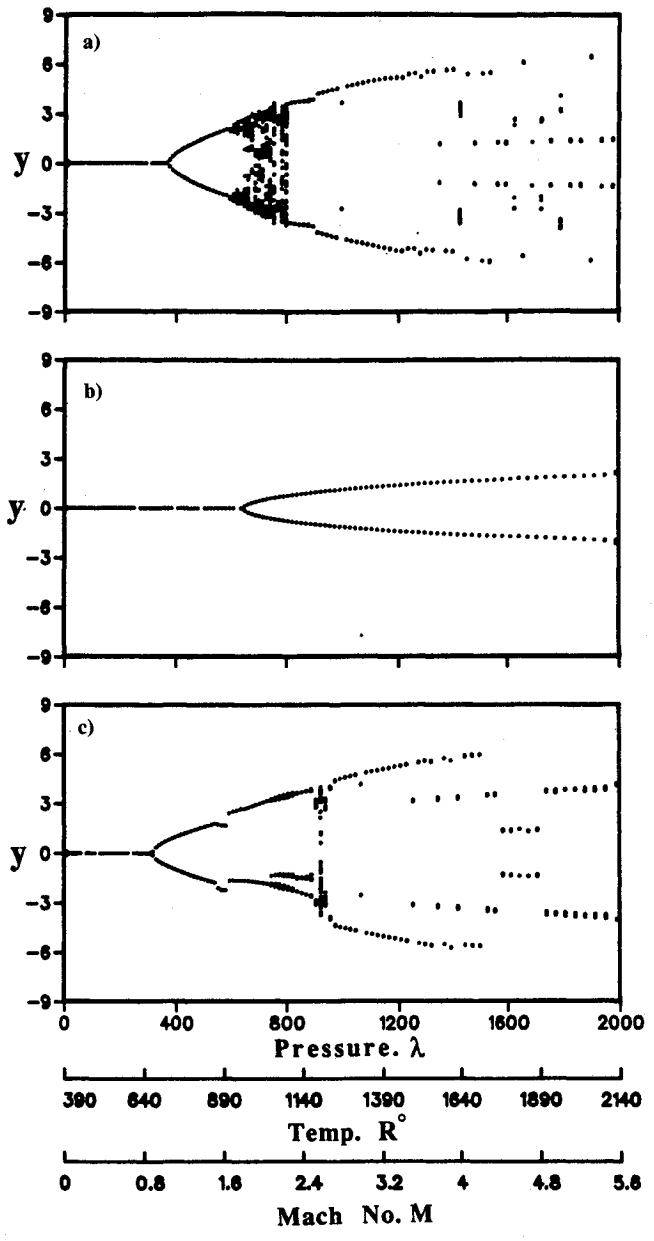

Fig. 11 Poincare sections of the first return as estimated by numerical integration for three different heated panels: a) isotropic panel (steel); b) orthotropic panel (graphite/epoxy) $\theta = 0$ deg; and c) orthotropic panel (graphite/epoxy) $\theta = 90$ deg.

proaches the buckling state. At aerodynamic pressure $\lambda = 795.0$ the motion becomes more regular, and the amplitude is drastically reduced for the first mode, whereas it is significantly amplified for the second and third modes as shown in Fig. 6. The frequency of oscillation is also much higher than the panel frequency at lower aerodynamic pressures as shown in Figs. 6 and 7. For 0-deg orthotropic heated panels, the first two modes oscillate sinusoidally with a phase shift of 180 deg as shown in Fig. 8. The amplitudes of the other modes are much smaller, and the panel oscillation is dominated by the first two modes. As the aerodynamic pressure increases, the amplitudes of all modes increase with irregular and random appearance of higher modes, e.g., modes 5 and 6. Under all possible dynamic pressures considered, the flutter is regular, and the amplitude of oscillation is relatively smaller than those of the isotropic and 90-deg orthotropic material. For 90-deg orthotropic material, the development of chaos is similar to that described for isotropic material. Figure 9 shows a set of time history records for the six modes just before chaotic motion takes place.

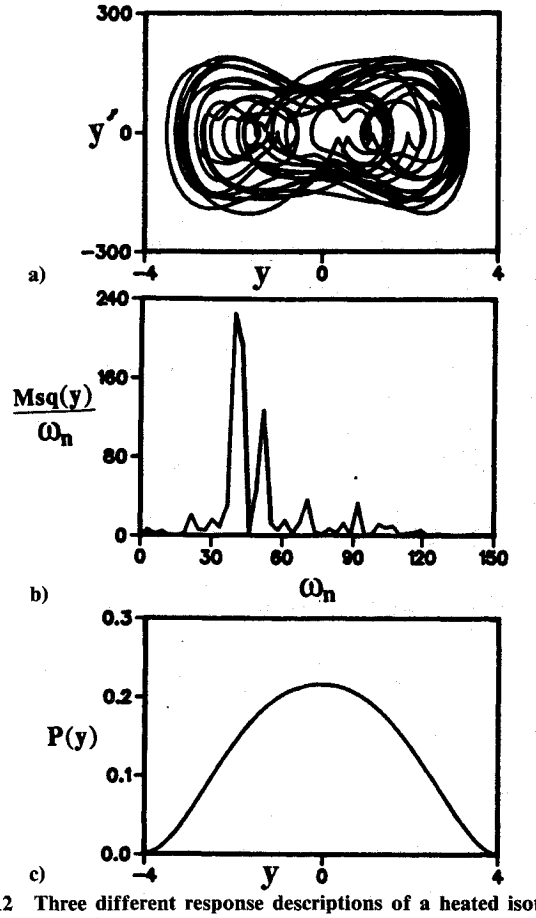

Fig. 12 Three different response descriptions of a heated isotropic panel ($T = 965°$R, $M = 1.85$, $\lambda = 665$): a) phase plane; b) power spectrum density; and c) probability density function.

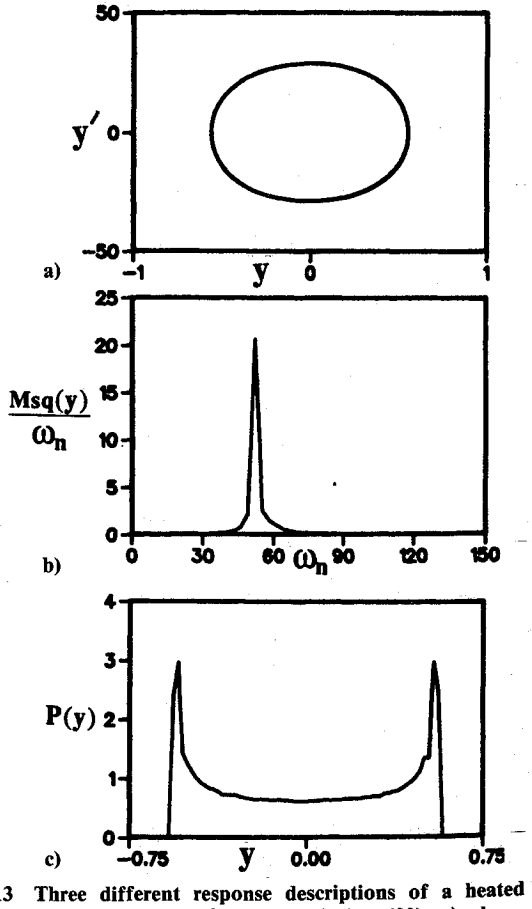

Fig. 13 Three different response descriptions of a heated 0-deg orthotropic panel ($T = 990°$R, $M = 1.8$, $\lambda = 680$): a) phase plane; b) power spectrum density; and c) probability density function.

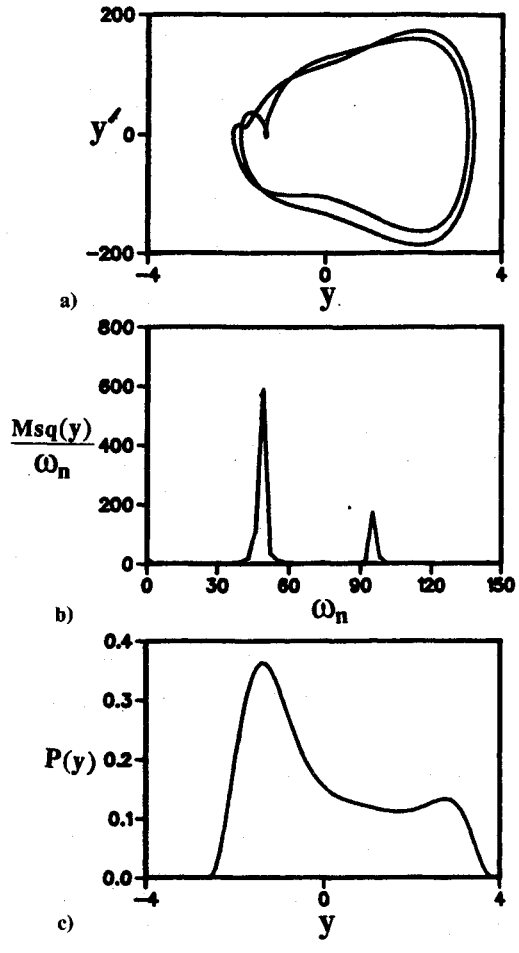

Fig. 14 Three different response descriptions of a heated 90-deg orthotropic panel ($T = 1030°$R, $M = 2.05$, $\lambda = 760$): a) phase plane; b) power spectrum density; and c) probability density function.

The dependence of the panel oscillation amplitude on the aerodynamic pressure is shown by the Poincare sections of the first return for the three types of unheated isotropic, 0-, and 90-deg orthotropic panel as in Figs. 10a–10c, respectively. For the isotropic unheated panel, Fig. 10a, the results are similar to those reported by Dowell.[24] Figure 11 shows similar curves for heated panels. Comparison of Figs. 10 and 11 reveals that the amplitudes of heated panels are significantly higher than those of unheated panels. In both heated and unheated cases, the 0-deg orthotropic panel does not experience any chaos. For heated isotropic panels, the degree of irregular motion is much greater than that of the 90-deg orthotropic panel.

Figures 12–14 show samples of panel characteristics in terms of phase portraits, power spectral density functions, and probability density functions. Figure 12 shows a typical set of response statistics for a heated isotropic panel where the response is purely random and its probability density is almost Gaussian. The power spectral density reveals several spikes, the first of which is located at a frequency $39.0\omega_0$ rad/s (where $\omega_0 = \sqrt{D_{11}/\bar{m}a^4}$), which is close to the first and second mode frequencies; the other is located at a frequency of $52.0\omega_0$ rad/s, which is close to the third and fourth mode frequencies. Figure 13 shows another sample of response behavior for a heated 0-deg orthotropic panel where the response is given by a smooth limit cycle with a typical sine wave probability density. The power spectral density is given by a spike at a frequency of $51.9\omega_0$ rad/s. Figure 14 shows the response statistics for a heated 90-deg orthotropic panel. It is seen that the probability density curve exhibits double maxima, which implies period doubling, or in nonlinear modern dynamics terminology is known as multifurcation. The power spectral density curve shows also two spikes at $49.0\omega_0$ and $95.0\omega_0$ rad/s.

Conclusions

The problem of aerothermoelasticity of three different panel materials exposed to high-speed airflow is investigated. The panel materials considered are isotropic (steel) and 0- and 90-deg orthotropic (graphite/epoxy). Linear modal analysis showed the possible existence of internal resonance conditions at critical values of aspect ratios that occur at the points of intersection of the dotted and solid curves of Fig. 2. However, both flutter analysis and nonlinear response characteristics were examined in the absence of internal resonance conditions. For simply supported panels and where only the interaction of the six modes is considered, it is shown that aerodynamic heating enhances the occurrence of flutter at lower aerodynamic pressure. Aerodynamic heating also results in panel buckling, especially for isotropic and 90-deg orthotropic panels. As the panel approaches the onset of buckling, the nonlinear response yields complex characteristics including period doubling and chaos. The development of chaos is examined in the time domain and in terms of statistical response parameters such as power spectra and probability density functions. The authors are currently studying related problems of aerothermoelasticity by considering other factors such as internal resonance conditions, rotary inertia and shear deformation, and the effect of viscous and structural damping on the heated panel response.

Appendix

Elements of $\bar{Q}$ matrix for a generally orthotropic lamina associated with the xy axes are

$$\bar{Q}_{11} = Q_{11}s^4 + 2(Q_{12} + 2Q_{66})s^2c^2 + Q_{22}c^4$$

$$\bar{Q}_{22} = Q_{11}c^4 + 2(Q_{12} + 2Q_{66})c^2s^2 + Q_{22}s^4$$

$$\bar{Q}_{12} = \bar{Q}_{21} = Q_{12}(s^4 + c^4) + (Q_{11} + Q_{22} - 4Q_{66})s^2c^2$$

$$\bar{Q}_{66} = (Q_{11} + Q_{22} - 2Q_{66} - 2Q_{12})s^2c^2 + Q_{66}(s^4 + c^4)$$

$$\bar{Q}_{16} = (Q_{11} - Q_{12} - 2Q_{66})c^3s + (Q_{12} - Q_{22} + 2Q_{66})cs^3$$

$$\bar{Q}_{26} = (Q_{11} - Q_{12} - 2Q_{66})s^3c + (Q_{12} - Q_{22} + 2Q_{66})sc^3$$

where Q_{ij} without the overbar belong to the principal material axes $12z$ and $s = \sin\theta$ and $c = \cos\theta$.

For a specially orthotropic panel, the Q_{ij} are related to the lamina constants by the following relations:

$$Q_{11} = \frac{E_{11}}{1 - \vartheta_{12}\vartheta_{12}}, \quad Q_{22} = \frac{E_{22}}{1 - \vartheta_{12}\vartheta_{12}}$$

$$Q_{12} = Q_{12} = \frac{E_{11}\vartheta_{21}}{1 - \vartheta_{12}\vartheta_{12}}, \quad Q_{66} = G_{12}, \quad Q_{16} = Q_{26} = 0.0$$

Similarly, the coefficients of the thermal expansion associated with the xy axes are

$$\alpha_x = (\cos\theta)^2\alpha_1 + (\sin\theta)^2\alpha_2, \quad \alpha_y = (\sin\theta)^2\alpha_1 + (\cos\theta)^2\alpha_2$$

$$\alpha_{xy} = 2(\alpha_1 - \alpha_2)\cos\theta\sin\theta$$

where α_1 and α_2 are the thermal expansion coefficients along the 1 and 2 axes, respectively.

Elements of $[A_{ij}]^{-1}$ matrix for a generally orthotropic lamina are

$$\bar{A}_{11} = A_{22}A_{66} - \frac{A_{26}^2}{\Delta 1}, \quad \bar{A}_{12} = A_{16}A_{26} - \frac{A_{12}A_{66}}{\Delta 1}$$

$$\bar{A}_{16} = A_{12}A_{16} - \frac{A_{22}A_{16}}{\Delta 1}, \quad \bar{A}_{22} = A_{11}A_{66} - \frac{A_{16}^2}{\Delta 1}$$

$$\bar{A}_{26} = A_{12}A_{16} - \frac{A_{11}A_{26}}{\Delta 1}, \quad \bar{A}_{66} = A_{11}A_{22} - \frac{A_{12}A_{21}}{\Delta 1}$$

$$\Delta 1 = A_{11}A_{22}A_{66} - A_{12}A_{12}A_{66} + A_{12}A_{26}A_{16} - A_{11}A_{26}A_{62} + A_{16}A_{12}A_{26} - A_{16}A_{22}A_{61}$$

where A_{ij} and D_{ij} are the extensional stiffness and bending stiffness matrices, respectively. The elements of A_{ij} and D_{ij} are given by

$$(A_{ij}, D_{ij}) = \sum_{k=1}^{n} \int_{z_{k-1}}^{z_k} (1, z^2)[\bar{Q}_{ij}]\, dz$$

References

[1]Bisplinghoff, R. L., and Dugundji, J., "Influence of Aerodynamic Heating on Aeroelastic Phenomena," *High Temperature Effects in Aircraft Structures,* edited by N. J. Hoff, Pergamon Press, New York, 1958, pp. 288–312.

[2]Houbolt, J. C., "A Study of Several Aerothermoelastic Problems of Aircraft Structures in High-Speed Flight," Mitteilungen Aus Dem Institut fur Flugzeugstatik und Leichtbau, No. 5, Verlag Leeman, Zurich, Switzerland, 1958.

[3]Fung, Y. C., "The Static Stability of a Two Dimensional Curved Panel in a Supersonic Flow with an Application to Panel Flutter," *Journal of the Aeronautical Sciences,* Vol. 21, No. 8, 1954, p. 556.

[4]Schaeffer, H. G., and Heard, W. L., "Supersonic Flutter of a Thermally Stressed Flat Panel with Uniform Edge Loads," NASA TN D-3077, Oct. 1965.

[5]Boley, B. A., "Thermally Induced Vibrations of Beams," *Journal of the Aeronautical Sciences,* Vol. 33, No. 2, 1965, pp. 179–181.

[6]Sylvester, M. A., "Experimental Studies of Flutter of Buckled Rectangular Panels at Mach Numbers From 1.2 to 3.0 Including Effects of Pressure Differential and of Panel Width-Length Ratio," NASA TN D-833, May 1961.

[7]Sylvester, M. A., and Baker, J. E., "Some Experimental Studies of Panel Flutter at Mach Number 1.3," NACA TN 3914, Feb. 1957.

[8]Sylvester, M. A., Nelson, H. C., and Cunningham, H. J., "Experimental and Theoretical Studies of Panel Flutter at Mach Numbers 1.2 to 3.0," NACA RM L55E18b, July 1955.

[9]Kordes, E. E., Tuovila, W. J., and Guy, L. D., "Flutter Research on Skin Panels," NASA TN D 451, Sept. 1960.

[10]Dixon, S. C., Griffith, G. E., and Bohen, H. L., "Experimental Investigation at Mach Number 3.0 of the Effects of Thermal Stress and Buckling on the Flutter of Four-Bay Aluminum Alloy Panels with Length-Width Ratios of 10," NASA TN D-921, Oct. 1961.

[11]Guy, L. D., and Bohon, H. L., "Flutter of Aerodynamically Heated Aluminum-Alloy and Stainless-Steel Panels with Length-Width Ratios of 10 at Mach No. of 3.0," NASA TN D-1353, July 1962.

[12]Reissner, E., and Stavsky, Y., "Bending and Stretching of Certain Types of Heterogenous Aeolotropic Elastic Plates," *ASME Journal of Applied Mechanics,* Vol. 28, No. 2, 1961, pp. 402–409.

[13]Leissa, A. W., "Vibration of Plates," NASA SP 160, 1969.

[14]Szilard, R., *Theory and Analysis of Plates, Classical and Numerical Methods,* Prentice-Hall, Englewood Cliffs, NJ, 1974, Chap. 4.

[15]Ashton, J. E., and Whitney, J. M., *Theory of Laminated Plates,* Vol. IV, Technomic Co., Stamford, CT, 1970, pp. 77–91.

[16]Chia, C. Y., *Nonlinear Analysis of Plates,* McGraw-Hill, New York, 1980, pp. 372–402.

[17]Bohon, H. L., "Flutter of Flat Rectangular Orthotropic Panels with Biaxial Loading and Arbitrary Flow Direction," NASA TN D-1949, Sept. 1963.

[18]Bohon, H. L., and Anderson, M., "Role of Boundary Conditions on Flutter of Orthotropic Panels," *AIAA Journal,* Vol. 4, No. 7, 1966, pp. 1241–1248.

[19]Ketter, D. J., "Flutter of Flat Rectangular Orthotropic Panels," *AIAA Journal,* Vol. 5, No. 1, 1967, pp. 116-124.

[20]Lee, I., and Cho, M. H., "Flutter Analysis of Composite Panels in Supersonic Flow," *Proceedings of the Structures, Structural Dynamics and Materials Conference* (Long Beach, CA), AIAA, Washington, DC, 1990, pp. 1540–1550 (AIAA Paper 90-1190-CP).

[21]Fung, Y. C., *Foundations of Solid Mechanics,* Prentice-Hall, Englewood Cliffs, NJ, 1965, pp. 292–300.

[22]Vinson, J. R., and Chou, T. W., *Composite Materials and Their Use in Structures,* Wiley, New York, 1975.

[23]Truitt, R. W., *Fundamentals of Aerodynamic Heating,* The Ronald Press Co., New York, 1960, pp. 202–239.

[24]Dowell, E. H., "Panel Flutter: A Review of Aeroelastic Stability of Plates and Shells," *AIAA Journal,* Vol. 8, No. 3, 1970, pp. 385-399.

[25]Hetnarski, R. B., *Thermal Stresses I,* North-Holland, Amsterdam, The Netherlands, 1986, pp. 100–130.

[26]Sun, C. T., and Chen, J. K., "Transient Thermal Stress Analysis in Graphite/Epoxy Composite Laminates," *Developments in Theoretical and Applied Mechanics,* Vol. 11, 1982, pp. 309-328.

[27]Chang, S. I., Bajaj, A. K., and Krousgrill, C. M., "Amplitude Modulated Dynamics in Harmonically Excited Nonlinear Oscillations of Rectangular Plates with Internal Resonance," *Structural Dynamics: Recent Advances,* edited by M. Petyt, H. F. Wolf, and C. Mei, Elsevier, New York, 1991, pp. 739–748.

[28]Ashley, H., and Zartarian, G., "Piston Theory—A New Aerodynamic Tool for the Aeroelastician," *Journal of the Aeronautical Sciences,* Vol. 23, No. 12, 1956, pp. 1109–1118.